2022 IEEE 61st Conference on Decision and Control (CDC)
December 6-9, 2022. Cancún, Mexico

A Discrete-Time Approach to Analysis of Sampled-Data Hybrid Integrator-Gain Systems

B. Sharif D.W.T. Alferink M.F. Heertjes H. Nijmeijer W.P.M.H. Heemels

2022 IEEE 61st Conference on Decision and Control (CDC) | 978-1-6654-6761-2/22/$31.00 ©2022 IEEE | DOI: 10.1109/CDC51059.2022.9992653

***Abstract*— Hybrid integrator-gain systems (HIGS) are hybrid control elements used to overcome fundamental performance limitations of linear time-invariant feedback control, and have enjoyed early engineering successes in mechatronic applications such as control of high-precision motion systems. However, the development of discretized versions of HIGS and their sampled-data analysis have not been addressed in the literature so far. This paper presents a discrete-time version of HIGS, which preserves the main philosophy behind the operation of HIGS in continuous time. Moreover, stability criteria are presented that can be used to certify input-to-state stability of discrete-time and sampled-data HIGS-controlled systems based on both (i) (measured) frequency response data, and (ii) linear matrix inequalities (LMIs). A numerical case study demonstrates the use of the main results.**

I. Introduction

Hybrid integrator-gain systems (HIGS) are hybrid control elements that have been shown to be effective tools in realizing performance beyond the limitations of linear time-invariant (LTI) control [18], [21]. Extensive research has led to several fruitful results for HIGS and HIGS-based control design in terms of mathematical formalization, well-posedness and stability analysis [3], [13], [14], [17], [19], overcoming fundamental limitations of LTI control [18], [21], and improving closed-loop performance of control systems [2], [5], [16], [20]. Thus far the literature related to HIGS, however, has not treated important aspects related to the development of discrete time versions of HIGS and analysis of sampled-data HIGS-based controllers, which we aim to address in this paper. Given that nowadays almost all controllers are implemented digitally, this forms an important topic of research for HIGS and HIGS-based control design.

Generally speaking, there exist three main approaches for the design of digital controllers for continuous-time (CT) plants. These are [11]: (i) the continuous-time design approach (abbreviated as CTD), in which CT controllers are designed based on a CT model of the plant and subsequently discretized and implemented (often at a high sampling rate); (ii) the discrete-time approach (abbreviated as DTD), in which a discrete-time (DT) controller is designed based on a DT model of the plant (ignoring the inter-sample behavior); and (iii) the sampled-data design approach (abbreviated as SDD), in which a discrete-time controller is designed based on a CT model of the plant (thus directly including the inter-sample behavior). All these approaches are of interest for sampled-data HIGS-based control. In this work, we focus on the DTD approach, which is typically easier to apply in practice compared to the SDD approach, and has the advantage of providing direct guarantees on DT closed-loop behavior (in contrast to the CTD approach) that, under appropriate conditions, can also be used to provide guarantees when taking the inter-sample behavior into account [12], as will be shown in this paper.

Our contributions are fourfold. As a first contribution, we present a DT version of HIGS, which preserves the essential characteristics and the main philosophy behind the operation of HIGS in continuous-time. We present two sets of stability criteria that can be used to certify input-to-state stability (ISS) of systems consisting of DT HIGS-based controllers and a DT LTI plant. These two sets of ISS criteria are based on (i) (measured) frequency response data, and (ii) linear matrix inequalities (LMIs), forming the second and third contributions of the paper, respectively. We also show that the LMIs are guaranteed to provide less conservative results compared to the frequency-domain criterion as satisfaction of the latter implies feasibility of a special case of the LMIs. As a fourth contribution, it is shown that DT ISS guarantees imply also ISS of sampled-data HIGS-controlled systems consisting of DT HIGS-based controllers and a CT LTI plant (including the inter-sample behavior). A numerical case study is also provided, to illustrate the results.

The remainder of the paper is organized as follows. Section II contains a short introduction to CT HIGS and its main motivation. Section III introduces DT HIGS. In Section IV the closed-loop system under consideration is described. Stability criteria in frequency and time-domain are presented in Sections V and VI, respectively. Section VII extends the DT stability analysis to sampled-data HIGS-controlled systems. This is followed by a numerical example and conclusions in Sections VIII and IX, respectively.

The following notation conventions will be used. We denote a real, symmetric matrix $A \in \mathbb{R}^{n\times n}$ by $A \in \mathbb{S}^{n\times n}$. Given a symmetric matrix $A \in \mathbb{S}^{n\times n}$ we say that it is positive (negative)-definite, denoted by $A \succ (\prec) 0$, if $x^\top Ax > (<)\, 0$ for all $x \in \mathbb{R}^n \setminus \{0\}$. We write $A \in \mathbb{S}^{n\times n}_{\geq 0}$, if A is symmetric and all its elements are non-negative. The inequality symbols $>,\ \geq,\ <,\ \leq$ for a vector are understood component-wise. For a vector $x \in \mathbb{R}^n$ we denote its p norm in $\mathbb{R}^n$ by $\|x\|_p$. We write $\|x\|$ for the standard Euclidean norm. For a matrix $A \in \mathbb{R}^{n\times m}$ we use $\|A\|_\infty = \max_{1\leq i\leq m} \sum_{j=1}^{n} |a_{ij}|$, where $|a_{ij}|$ denotes the absolute value of the element in the i^{th} row and j^{th} column of A. For a bounded function $u : \mathbb{R}_{\geq 0} \to \mathbb{R}^n$, we write $\|u\|_\infty = \sup_{t\in\mathbb{R}_{\geq 0}} \|u(t)\|$. Similarly

Bardia Sharif, Dirk Alferink, Marcel Heertjes, Henk Nijmeijer, and Maurice Heemels are with the Department of Mechanical Engineering, Eindhoven University of Technology, The Netherlands. Marcel Heertjes is also with ASML Mechatronic Systems Development, Veldhoven, the Netherlands. E-mail corresponding author: b.sharif@tue.nl

This work has received funding as part of the project CLOC, which is financed by the Netherlands organization for scientific research (NWO). Maurice Heemels received funding from the European Research Council under the Advanced ERC Grant Agreement PROACTHIS, no. 101055384.

for a bounded function $w : \mathbb{N} \to \mathbb{R}^n$ we use the notation $\|w\|_\infty = \sup_{k\in\mathbb{N}}\|w(k)\|$.

II. Continuous-time HIGS

A CT HIGS element [2], denoted by $\mathscr{H}$, is described by

$$\mathscr{H}: \begin{cases} \dot{x}_h(t) = \omega_h e(t) & \text{if } (e(t), u(t), \dot{e}(t)) \in \mathscr{F}_1, \quad (1a) \\ x_h(t) = k_h e(t) & \text{if } (e(t), u(t), \dot{e}(t)) \in \mathscr{F}_2, \quad (1b) \\ u(t) = x_h(t) & \quad (1c) \end{cases}$$

with state $x_h(t) \in \mathbb{R}$, input $e(t) \in \mathbb{R}$, time-derivative $\dot{e}(t) \in \mathbb{R}$ of the input, and output $u(t) \in \mathbb{R}$, at time $t \in \mathbb{R}_{\geq 0}$. The parameters $\omega_h \in [0, \infty)$, $k_h \in (0, \infty)$ denote the integrator frequency and the gain parameter of the HIGS element, respectively. Moreover, $\mathscr{F}_1$ and $\mathscr{F}_2$ denote the regions in $\mathbb{R}^3$, where the different subsystems are active. A HIGS element primarily operates in the so-called integrator mode (1a). However, the integrator mode dynamics can only be followed as long as the input-output pair (e, u) of $\mathscr{H}$ remains inside the sector

$$\mathcal{S} := \left\{ (e, u) \in \mathbb{R}^2 \mid eu \geq \frac{1}{k_h} u^2 \right\}. \tag{2}$$

When the pair (e, u) tends to leave $\mathcal{S}$, a switch is made to the so-called gain mode (1b), keeping the trajectories on the sector boundary, where $u = k_h e$, and thus in $\mathcal{S}$. In particular, the sets $\mathscr{F}_1$ and $\mathscr{F}_2$, are given by

$$\mathscr{F}_1 := \{(e, u, \dot{e}) \in \mathbb{R}^3 \mid (e, u) \in \mathcal{S}\} \setminus \mathscr{F}_2, \tag{3}$$

$$\begin{aligned} \mathscr{F}_2 :=& \{(e, u, \dot{e}) \in \mathbb{R}^3 \mid (e, u) \in \mathcal{S} \wedge u = k_h e \\ & \wedge \omega_h e^2 > k_h \dot{e} e\}. \end{aligned} \tag{4}$$

As a result of this construction, the input and output of a HIGS element have the same sign at all times, and, even more, the input and output remain inside the set $\mathcal{S}$ as defined in (2). This leads to favorable properties in terms of a reduced phase lag of 38.15 degrees from a describing function perspective [3], in contrast to the 90 degrees phase lag of a standard linear integrator. In [18], [21], it was shown how these features of sign equivalence can be used to overcome fundamental overshoot performance limitations present in LTI control, making HIGS a promising control element. Additionally, HIGS has been shown to offer performance enhancing properties, for applications such as high-precision mechatronics [2], [16], [20], and active vibration isolation systems [5].

III. Discrete-Time HIGS

In this section we introduce a DT HIGS, which preserves the main characteristics of CT HIGS, and is given by

$$\overline{\mathscr{H}}: \begin{cases} x_h[k] = x_h[k-1] + \omega_h T_s e[k] & \text{if } \tilde{\xi}[k] \in \tilde{\mathscr{F}}_1, \quad (5a) \\ x_h[k] = k_h e[k] & \text{if } \tilde{\xi}[k] \in \tilde{\mathscr{F}}_2, \quad (5b) \\ u[k] = x_h[k] & \quad (5c) \end{cases}$$

where $e[k] \in \mathbb{R}$, $x_h[k] \in \mathbb{R}$, and $u[k] \in \mathbb{R}$ denote the input, state and output of the system, respectively, at time instant $t = kT_s$, with $k \in \mathbb{N}$ the discrete time-step, and $T_s \in \mathbb{R}_{>0}$ the sampling period. The decision of which mode of operation is active is based on the decision variable $\tilde{\xi}[k] := (e[k], u^-[k], e^-[k]) := (e[k], u[k-1], e[k-1])$, while the regions where different subsystems are active, are denoted by $\tilde{\mathscr{F}}_1,\ \tilde{\mathscr{F}}_2 \subseteq \mathbb{R}^3$, which will be specified below.

The DT integrator mode dynamics are given by (5a), obtained by backward Euler discretization of (1a). Moreover, the DT gain mode dynamics are given by (5b). Note that since (1a) has integrator dynamics, both its backward and forward Euler integration are exact with respect to the integration of the state (since $e^0 = I$), and thus, the choice between backward and forward Euler discretization, only influences the approximation of the input term used on the right-hand-side of (5a), i.e., $e[k]$ for backward Euler and $e[k-1]$ for forward Euler.

As in the case of CT HIGS, given an input e, a DT HIGS element is designed to primarily operate in the integrator mode (5a), while generating an output u such that $(e[k], u[k]) \in \mathcal{S}$, for all $k \in \mathbb{N}$, with $\mathcal{S}$ as defined in (2). We assume that $(e[0], u[0]) \in \mathcal{S}$, which, given $e[0]$, can always be arranged by a proper choice of $x_h[0] = u[0]$ (e.g., $x_h[0] = u[0] = 0$ is always a viable choice). At moments when the integrator mode dynamics lead to trajectories that would violate (2), a switch is made to the other mode such that the resulting input-output pair $(e[k], u[k]) \in \mathcal{S}$, for all $k \in \mathbb{N}$. To capture this philosophy, we define

$$\begin{aligned} \tilde{\mathscr{F}}_1 :=& \{\tilde{\xi} \in \mathbb{R}^3 \mid (e^-, u^-) \in \mathcal{S} \wedge \\ & (u^- + \omega_h T_s e) e \geq \frac{1}{k_h} (u^- + \omega_h T_s e)^2\} \end{aligned} \tag{6}$$

as the region where the integrator mode dynamics (5a) are active. Note that the second condition defining the set in (6) uses a one-step ahead prediction of the output u, according to the integrator mode dynamics (5a). In particular, with $\tilde{\mathscr{F}}_1$ as defined in (6), given $(e[k-1], u[k-1]) \in \mathcal{S}$ and a new sample $e[k]$ of the input, the integrator mode dynamics are active, if the output $u[k]$ to be generated by operation in the integrator mode satisfies $(e[k], u[k]) \in \mathcal{S}$, as computed in $(u^- + \omega_h T_s e) e \geq \frac{1}{k_h} (u^- + \omega_h T_s e)^2$, in (6).

Using a similar reasoning as above, the region where the gain mode dynamics are active is chosen as the complement

$$\begin{aligned} \tilde{\mathscr{F}}_2 :=& \{\tilde{\xi} \in \mathbb{R}^3 \mid (e^-, u^-) \in \mathcal{S} \\ & \wedge (u^- + \omega_h T_s e) e < \frac{1}{k_h} (u^- + \omega_h T_s e)^2\}, \end{aligned} \tag{7}$$

as it results in operation in the gain mode (5b) only if the trajectories resulting from the integrator mode (5a) would violate (2). With the choice of sets $\tilde{\mathscr{F}}_1$ and $\tilde{\mathscr{F}}_2$ as in (6) and (7), the DT HIGS element (5) predominantly operates in the integrator mode and generates an output u such that $(e[k], u[k]) \in \mathcal{S}$, for all $k \in \mathbb{N}$, thereby preserving the main philosophy behind the operation of CT HIGS (1).

An illustration of the regions $\tilde{\mathscr{F}}_1$, and $\tilde{\mathscr{F}}_2$, when $k_h = \omega_h = 1,\ T_s = 0.5$, is provided in Fig. 1. Note that while the gain mode dynamics (1b) of a CT HIGS element are active on a lower-dimensional subspace of the $(e, u, \dot{e})$ space (due to the condition $u = k_h e$ in (4)), as shown in Fig. 1, both modes of (5) are active on sets with non-empty interiors.

In the next section we describe the use of DT HIGS in a DT control setting (with a DT plant) and analyse this system

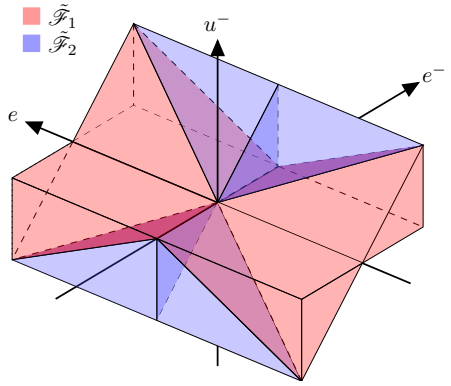

Fig. 1: Regions $\tilde{\mathscr{F}}_1$, and $\tilde{\mathscr{F}}_2$, in the (e, u^-, e^-) space.

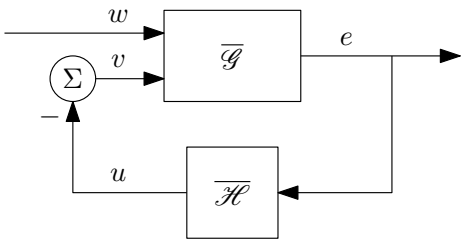

Fig. 2: HIGS-controlled closed-loop system.

in Sections V and VI, after which we discuss the sampled-data control setting (including the inter-sample behavior) with CT plants in Section VII.

IV. DT Closed-Loop System Description

We consider the closed-loop system in Fig. 2, consisting of a DT LTI system $\overline{\mathscr{G}}$ and a DT HIGS $\overline{\mathscr{H}}$, as described in (5). Here, $\overline{\mathscr{G}}$ contains the linear part of the loop, consisting of the plant to be controlled and possibly LTI parts of the controller. The system $\overline{\mathscr{G}}$ is given by

$$\overline{\mathscr{G}}: \begin{cases} x_g[k] &= A_g x_g[k-1] + B_{gv} v[k-1] + B_{gw} w[k-1], \\ e[k] &= C_g x_g[k] \end{cases} \tag{8}$$

with state $x_g[k]$ taking values in $\mathbb{R}^{n_g}$, output $e[k]$ taking values in $\mathbb{R}$, control input $v[k]$ in $\mathbb{R}$ and exogenous disturbances $w[k]$ in $\mathbb{R}^{n_w}$, $k \in \mathbb{N}$. Moreover, A_g, B_{gv}, B_{gw}, and C_g are real matrices of appropriate dimensions. For the closed-loop interconnection in Fig. 2, we have the state $x[k] = [x_g^\top[k]\ x_h^\top[k]]^\top \in \mathbb{R}^n$, where $n = n_g + 1$. By combining (5) and (8), we arrive at the state-space representation

$$\Sigma: \begin{cases} x[k] = A_i x[k-1] + B_i w[k-1], \ \text{if } \tilde{\xi}[k] \in \tilde{\mathscr{F}}_i, i \in \{1,2\} \\ e[k] = Cx[k], \end{cases} \tag{9}$$

for the closed-loop dynamics with

$$\left[\begin{array}{c|c} A_1 & B_1 \end{array}\right] = \left[\begin{array}{cc|c} A_g & -B_{gv} & B_{gw} \\ \omega_h T_s C_g A_g & 1 - \omega_h T_s C_g B_{gv} & \omega_h T_s C_g B_{gw} \end{array}\right], \tag{10}$$

$$\left[\begin{array}{c|c} A_2 & B_2 \end{array}\right] = \left[\begin{array}{cc|c} A_g & -B_{gv} & B_{gw} \\ k_h C_g A_g & -k_h C_g B_{gv} & k_h C_g B_{gw} \end{array}\right], \tag{11}$$

$$C = \left[\begin{array}{cc} C_g & 0 \end{array}\right]. \tag{12}$$

We study the stability of (9) in the next sections. In doing so, we adopt the notion of input-to-state stability (ISS) as defined in Definition 4.1 below.

Definition 4.1: [1] [7] System (9) is said to be input-to-state stable (ISS) with respect to w, if there exist a $\mathcal{KL}$-function $\beta : \mathbb{R}_{\geq 0} \times \mathbb{R}_{\geq 0} \to \mathbb{R}_{\geq 0}$ and a $\mathcal{K}$-function γ such that, for each bounded input $w : \mathbb{N} \to \mathbb{R}^{n_w}$ and each initial condition x_0, it holds that

$$\|x(k, x_0, w)\| \leq \beta(\|x_0\|, k) + \gamma(\|w\|_\infty),$$

for each $k \in \mathbb{N}$, where $x(k, x_0, w)$ denotes the trajectory of system (9), with initial state x_0 and input w at discrete-time instant k.

V. Frequency-Domain Stability Conditions

In this section results are presented, which guarantee ISS of (9), using simple-to-check graphical conditions based on frequency response functions of the plant model (8). As frequency response functions are generally easy to measure in practice (e.g., in mechatronic positioning systems), such frequency-based conditions for ISS, are appealing to control practitioners.

Theorem 5.1: Consider system (9) with (A_g, B_{gv}, C_g) being a minimal realization. The system is ISS, if

(i) The system matrix A_g is Schur;
(ii) $\frac{1}{k_h} + \mathrm{Re}\{W(z)\} > 0$, for all $z \in \mathbb{C}$, $|z| = 1$, with

$$W(z) = C_g(zI - A_g)^{-1} B_{gv}. \tag{13}$$

The conditions in Theorem 5.1, resemble the Tsypkin criterion [9], which is the DT analog of the CT circle criterion [8], for the study of DT absolute stability. However, while the Tsypkin criterion is concerned with static, memory-less nonlinearities, DT HIGS is a dynamical system, thereby requiring additional steps and arguments in the proof.

Theorem 5.1 can be verified using easy-to-measure frequency response functions (FRFs). In particular, condition (i) can be checked using standard linear control arguments. For a given value of $k_h \in \mathbb{R}_{>0}$, checking condition (ii), boils down to checking whether the Nyquist plot of $W(e^{j\omega})$ lies to the right of the vertical line passing through the point $\frac{-1}{k_h} + j0$ in the complex plane, for all $\omega \in [0, 2\pi]$. Therefore, checking the conditions in Theorem 5.1 does not require an analytical model of the plant, which can be hard to obtain in practice.

VI. Time-Domain Stability analysis

In this section we present LMI-based conditions that guarantee ISS of (9), using a multiple Lyapunov function approach [4]. We exploit the fact that the input-output pair of the proposed DT HIGS (5) satisfies (2), for all $k \in \mathbb{N}$. In particular, we partition the input-output space of DT HIGS (5) and allow different Lyapunov functions to be active within each region of the partition. The partitioning

[1] A continuous function $\alpha : [0, \infty) \to [0, \infty)$ is said to belong to class $\mathcal{K}$, if it is strictly increasing and $\alpha(0) = 0$. A continuous function $\beta : [0, \infty) \times [0, \infty) \to [0, \infty)$ is said to belong to class $\mathcal{KL}$, if for each fixed s, the mapping $r \mapsto \beta(r, s)$ belongs to class $\mathcal{K}$ and, for each fixed r, the mapping $s \mapsto \beta(r, s)$ is decreasing and $\beta(r, s) \to 0$ as $s \to \infty$.

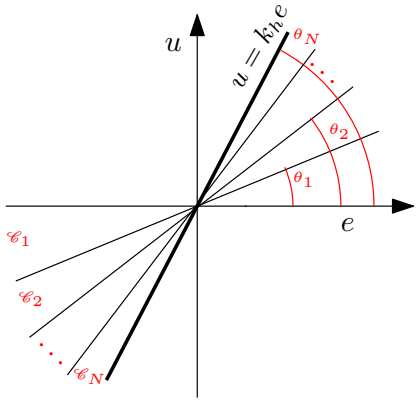

Fig. 3: Partitioning of the input-output space of DT HIGS.

employed in this work is similar to the one used in [20], [22] for reset control systems and CT HIGS-controlled systems. More specifically, the input-output $e-u$ plane is partitioned into N sub-sectors $\mathscr{C}_i$, $i \in \{1, 2, \dots, N\}$, by choosing $N+1$ equidistantly spaced angles $0 = \theta_0 < \theta_1 < \cdots < \theta_N = \arctan(k_h)$, as shown in Fig. 3. Loosely speaking, $\mathscr{C}_i$ is related to the sector $[\theta_{i-1}, \theta_i]$ in the $e-u$ plane. As shown in [20], [22], for every pair (e, u) located in $\mathscr{C}_i$ one has

$$\underbrace{\begin{bmatrix} -\sin\theta_{i-1} & \cos\theta_{i-1} \\ \sin\theta_i & -\cos\theta_i \end{bmatrix}}_{E_i} \begin{bmatrix} e \\ u \end{bmatrix} \geq 0 \tag{14}$$

for all (e, u) in the first quadrant of the $e-u$ plane, and $E_i \begin{bmatrix} e \\ u \end{bmatrix} \leq 0$, for all (e, u) in the third quadrant of the $e-u$ plane. Moreover, let us note that

$$\begin{bmatrix} e[k] \\ u[k] \end{bmatrix} = \underbrace{\begin{bmatrix} C_g & 0 \\ 0 & 1 \end{bmatrix}}_{\overline{C}} \begin{bmatrix} x_g[k] \\ x_h[k] \end{bmatrix}. \tag{15}$$

Therefore, $(e, u) \in \mathscr{C}_i$, $i \in \{1, 2, \dots, N\}$, translates on the level of states to $x \in \mathcal{S}_i$, $i \in \{1, 2, \dots, N\}$, with

$$\mathcal{S}_i = \{x \in \mathbb{R}^n \mid E_i \overline{C} x \geq 0 \vee E_i \overline{C} x \leq 0\} \tag{16}$$

with E_i and $\overline{C}$ defined as in (14) and (15), respectively.

Note that while a CT HIGS element (1) operates in the gain mode (1b) when $u = k_h e$ (see (4)) and thus x lies on the boundary of $\mathcal{S}_N$, a DT HIGS (5) can operate in both the integrator mode (5a) as well as the gain mode (5b) when $x \in \mathcal{S}_i$, for all $i \in \{1, ..., N\}$. However, after operation in the gain mode, the trajectories do lie on the boundary of $\mathcal{S}_N$. Moreover, another subtlety that arises in the DT setting is that due to the DT nature of the dynamics, the solutions to the system can jump over sub-sectors, e.g., at $t = kT_s$ $x[k] \in \mathcal{S}_1$, and at $t = (k+1)T_s$, $x[k+1] \in \mathcal{S}_3$. Such a scenario is not encountered in CT due to the continuous evolution of solutions.

Theorem 6.1: Consider the system in (9). Suppose there exist symmetric matrices $W_i, U_{1,ij}, U_{2,i}, Y_{1,ij}, Y_{2,i} \in \mathbb{S}^{2\times 2}_{\geq 0}$ and $P_i \in \mathbb{S}^{n\times n}$, for $i, j \in \{1, 2, \dots, N\}$, such that

$$P_i - \overline{C}^\top E_i^\top W_i E_i \overline{C} \succ 0, \tag{17}$$

$$A_1^\top (P_j + \overline{C}^\top E_j^\top Y_{1,ij} E_j \overline{C}) A_1 - P_i + \overline{C}^\top E_i^\top U_{1,ij} E_i \overline{C} \prec 0, \tag{18}$$

$$A_2^\top (P_N + \overline{C}^\top E_N^\top Y_{2,i} E_N \overline{C}) A_2 - P_i + \overline{C}^\top E_i^\top U_{2,i} E_i \overline{C} \prec 0. \tag{19}$$

Then the closed-loop system (9) is ISS.

The strength of Theorem 5.1 lies in the fact that it can be verified based on graphical evaluations of FRF measurements. However, this Theorem only makes use of sector boundedness of the input-output pair of the HIGS element $\overline{\mathscr{H}}$ and does not exploit specific knowledge related to the internal dynamics of the HIGS element, making it possibly conservative. Moreover, Theorem 5.1 concludes stability of the closed-loop system on the basis of the existence of a common quadratic Lyapunov function. Theorem 6.1 on the other hand, makes extensive use of specific knowledge related to the internal HIGS dynamics and conclude stability on the basis of the existence of multiple Lyapunov functions. Consequently, Theorem 5.1. The downside of the LMI-based stability conditions with respect to the frequency domain condition is that they rely on parametric models of the underlying system which are not always easy to obtain. Additionally, in case the LMIs are infeasible, it is not clear how the controller parameters should be tuned to render the LMIs feasible.

We now state a result relating the satisfaction of the frequency-domain conditions in Theorem 5.1 to the feasibility of the LMIs in Theorem 6.1.

Theorem 6.2: Under minimality of (A_g, B_{gv}, C_g), satisfaction of the conditions in Theorem 5.1 implies feasibility of the LMIs in Theorem 6.1 with $N = 1$, $W_i = Y_{1,ij} = Y_{2,i} = 0_{2\times 2}$, $U_{1,ij} = U_{2,i} = U = \frac{1}{\alpha}\begin{bmatrix} 0 & 1 \\ 1 & 0 \end{bmatrix}$, and $P = \begin{bmatrix} P_g & 0 \\ 0 & \mu \end{bmatrix}$, where $P_g \in \mathbb{S}^{n_g \times n_g}$ is a positive-definite matrix and $\mu \in \mathbb{R}_{>0}$, $\alpha = \sin(\arctan(k_h))$.

As a result of Theorem 6.2, Theorem 5.1 will yield more conservative results compared to Theorem 6.1, due to certifying ISS on the basis of the existence of a common quadratic Lyapunov function (with a particular structure), as well as the particular choice of the S-procedure relaxations.

VII. Sampled-Data ISS Guarantees

In the previous sections, stability criteria were presented that can be used to guarantee ISS for closed-loop HIGS-controlled systems in DT (ignoring inter-sample behavior). In this section we show that DT ISS, implies ISS of sampled-data HIGS-controlled systems, thus also taking into account the inter-sample behavior, building on ideas in [15]. Consider the interconnection in Fig. 4 consisting of a CT linear plant $\mathscr{P}$, and a general DT nonlinear controller ϕ (e.g., a HIGS-based controller), interconnected via a sampler and a zero-order hold device.

Here, the plant is given by

$$\mathscr{P}: \begin{cases} \dot{x}_p(t) = \mathcal{A}_p x_p(t) + \mathcal{B}_{pu} u_p(t) + \mathcal{B}_{pd} d(t), \\ y(t) = \mathcal{C}_p x_p(t) \end{cases} \tag{20}$$

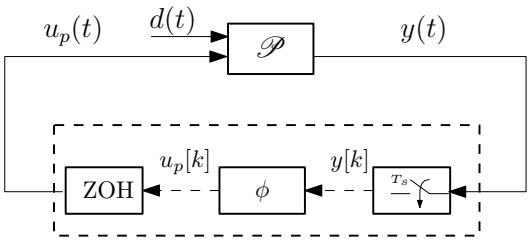

Fig. 4: CT plant $\mathscr{P}$ and sampled-data nonlinear controller.

with $\mathcal{A}_p$, $\mathcal{B}_{pu}$, $\mathcal{B}_{pd}$, $\mathcal{C}_p$ real matrices of appropriate dimensions, $x_p(t) \in \mathbb{R}^{n_p}$ the state of the plant, $u_p(t) \in \mathbb{R}^{n_u}$ and $d(t) \in \mathbb{R}^{n_d}$ the control input and the input disturbances, respectively, and $y(t) \in \mathbb{R}^{n_y}$ the plant output, at time $t \in \mathbb{R}_{\geq 0}$. The nonlinear controller ϕ is of the general form

$$\phi : \begin{cases} x_\phi[k] = f(y[k], y[k-1], x_\phi[k-1]), \\ u_p[k] = h(x_\phi[k]) \end{cases} \tag{21}$$

with $x_\phi[k] \in \mathbb{R}^{n_\phi}$, $u_p[k] \in \mathbb{R}^{n_u}$, $y[k] \in \mathbb{R}^{n_y}$ denoting its state, output and input, respectively, and $f : \mathbb{R}^{n_y} \times \mathbb{R}^{n_y} \times \mathbb{R}^{n_\phi} \to \mathbb{R}^{n_\phi}$, $h : \mathbb{R}^{n_\phi} \to \mathbb{R}^{n_y}$, at discrete time $k \in \mathbb{N}$, corresponding to time instants $t = kT_s$ with T_s the sampling period, as before. Note that the class of systems described by (21) includes as a particular case, HIGS-based controllers as shown in Fig. 5, consisting of a DT HIGS element (5) and DT LTI controllers $\mathcal{C}_i$, $i \in \{1, 2, 3\}$. Analysis of the system

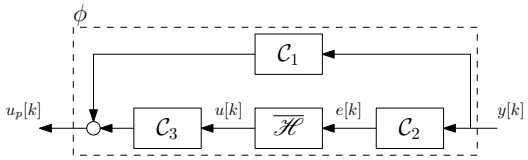

Fig. 5: The controller ϕ in the case of HIGS-based control.

in Fig. 4 by following the DTD approach (cf. Sections V and VI), requires a DT model of the plant $\mathscr{P}$ (20), which can be obtained via exact ZOH discretization of (20), leading to

$$\overline{\mathscr{P}} : \begin{cases} x_p[k] &= A_p x_p[k-1] + B_p u_p[k-1] + w[k-1], \\ y[k] &= C_p x_p[k] \end{cases} \tag{22}$$

with $A_p := e^{\mathcal{A}_p T_s}$, $B_p := \int_0^{T_s} e^{\mathcal{A}_p \tau} d\tau \mathcal{B}_{pu}$, $w[k-1] := \int_{(k-1)T_s}^{kT_s} e^{\mathcal{A}_p (kT_s - \tau)} \mathcal{B}_{pd} d(\tau) d\tau$, $C_p := \mathcal{C}_p$. Considering (22), we obtain the exact DT model

$$\begin{aligned} x_{sd}[k] &= \begin{bmatrix} A_p x_p[k-1] + B_p h(x_\phi[k-1]) + w[k-1] \\ f(C_p x_p[k], C_p x_p[k-1], x_\phi[k-1]) \end{bmatrix}, \\ y[k] &= \begin{bmatrix} C_p & 0 \end{bmatrix} x_{sd}[k] \end{aligned} \tag{23}$$

with $x_{sd}[k] = \begin{bmatrix} x_p^\top[k] & x_\phi^\top[k] \end{bmatrix}^\top$ for the system in Fig. 4. Using this exact model, we can formulate a corollary of Theorem 6 in [12], which can be used for concluding (CT) ISS of the sampled-data system under consideration, based on DT ISS of (23). See [15] for definition of ISS for CT systems.

Corollary 7.1: Suppose the DT system (23) is ISS with respect to the DT disturbance w. Then, the sampled-data system in Fig. 4, is ISS with respect to the CT disturbance d.

For the case where ϕ is a HIGS-based controller as in Fig. 5, (23) is given by (9). Thus, as a result of Corollary 7.1, one may conclude ISS of the resulting sampled-data HIGS-controlled system using Theorem 5.1 and Theorem 6.1.

Remark 7.1: For a stabilizing controller of (20) to exist, stabilizability of $(\mathcal{A}_p, \mathcal{B}_{pu})$ as well as detectability of $(\mathcal{A}_p, \mathcal{C}_p)$ are required [6]. Moreover, as shown in [1], [10], in order to avoid the loss of these properties as a result of sampling, and thus for the existence of a DT stabilizing controller of (20), the sampling period T_s should be non-pathological (see [1], [10] for a detailed explanation on this topic) with respect to $\mathcal{A}_p$. As such, these conditions are necessary for the satisfaction of the stability criteria in Sections V and VI.

VIII. Numerical Example

Consider the interconnection in Fig. 4, where $\mathscr{P}$ is a mass-spring-damper system with transfer function

$$\mathscr{P}(s) = \frac{1}{ms^2 + bs + k}, \tag{24}$$

and mass $m = 1$ kg, damping coefficient $b = 0.0564$ Ns/m and stiffness coefficient $k = 1$ N/m. Moreover, the controller ϕ is as depicted in Fig. 5, with $\mathcal{C}_1(z) = 0$, $\mathcal{C}_2(z) = 1$ and $\mathcal{C}_3(z) = C(z)$ a linear lead filter, obtained by discretization of $C(s) = 1.4\frac{s+5}{s+6.95}$, using zero-pole matching. Let us first consider a sampling time of $T_s = 0.001s$ (also used for the discretization of $C(s)$). To evaluate ISS of the DT closed-loop system using Theorem 5.1, note that the poles of the linear part of the system $P_{\text{lin}}(z) = P(z)C(z)$, with $P(z)$ the ZOH discretization of (24), are within the unit circle and thus condition (i) in Theorem 5.1 is satisfied. Checking

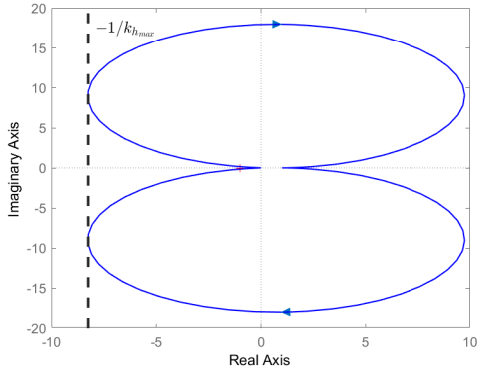

Fig. 6: Nyquist diagram of $P(z)C(z)$.

the condition (ii) in Theorem 5.1, amounts to inspecting the Nyquist diagram of $P_{\text{lin}}(e^{j\omega})$ as shown in Fig. 6, from which it follows that the closed-loop system is guaranteed to be ISS for any $\omega_h \in (0, \infty)$ and $k_h \leq 0.12$, by Theorem 5.1. Indeed, 0.12 is the maximal k_h value for which the Nyquist diagram in Fig. 6 falls to the right side of the vertical line passing through $\frac{-1}{k_h} + j0$, in the complex plain, and thus satisfies condition (ii) in Theorem 5.1. In addition, the results obtained from Theorem 6.1 using LMI-based ISS guarantees,

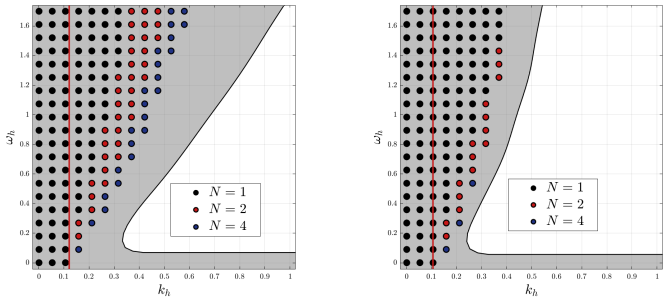

(a) (b)

Fig. 7: ISS region found by time-series simulations ■, ISS (k_h, ω_h) values returned by Theorem 6.1 (as a function of the number of partitions N), the k_h value obtained from Theorem 5.1 —, for a sampling time of (a) $T_s = 0.001s$, and (b) $T_s = 0.25s$.

are portrayed in Fig. 7a as a function of the number N of partitions, $N \in \{1, 2, 4\}$. Note that Fig. 7a also shows the range of parameters for which the system is estimated to be ISS based on extensive time-series simulations. As it can be seen in Fig. 7a, by using Theorem 6.1, one concludes stability of (9) for a range of (k_h, ω_h) well beyond the values found by application of the frequency-domain conditions in Theorem 5.1. This is indeed expected as a result of Theorem 6.2.

To illustrate the effect of the sampling period, Fig. 7b portrays the analysis results obtained with a sampling time of $T_s = 0.25s$. Note that for $T_s = 0.25s$, the simulation-based estimated ISS region (the grey area) is considerably smaller than for $T_s = 0.001s$. This indicates the general need for the analysis tools presented in this paper as pure CT analysis (see for example [3]) completely ignores the role of sampling, which in turn could cause wrong conclusions regarding stability. Let us also make the observation that even with a single quadratic Lyapunov function, i.e., for $N = 1$, Theorem 6.1 provides a feasible range of (k_h, ω_h) values extending well beyond those obtained by Theorem 5.1, which indicates the strength of the relaxation terms introduced in Theorem 6.1.

IX. Conclusions

We have proposed a DT version of HIGS, which preserves the main characteristics of CT HIGS, namely predominant operation in the integrator mode while guaranteeing sign equivalence (sector boundedness) of its input-output pair. For this DT HIGS element we have presented novel stability criteria that can be used to conclude ISS using (i) (measured) frequency response conditions and (ii) LMI-based conditions. We have also shown that satisfaction of these stability criteria imply ISS of sampled-data systems consisting of a CT plant and DT HIGS-based controllers (including the inter-sample behavior). While the frequency-domain criteria do not require parametric models and can be evaluated using easy-to-obtain frequency response data, we have formally proven that their satisfaction implies feasibility of a special case of the LMI-based conditions and thus are more conservative. This has been further illustrated by a numerical example showing that the LMIs are significantly less conservative than the frequency-domain criteria. Future research directions include reduction of the conservatism associated with the stability analysis, as well as transforming the presented stability criteria for synthesis of sampled-data HIGS-based controllers.

References

[1] T. Chen and B. Francis. *Optimal sampled-data control systems*. Springer, 1995.

[2] D. Deenen, M. F. Heertjes, M. Heemels, and H. Nijmeijer. Hybrid integrator design for enhanced tracking in motion control. In *American Control Conference*, pages 2863–2868, 2017.

[3] D. Deenen, B. Sharif, S. van den Eijnden, H. Nijmeijer, M. Heemels, and M. F. Heertjes. Projection-Based Integrators for Improved Motion Control: Formalization, Well-posedness and Stability of Hybrid Integrator-Gain Systems. 133:109830, 2021.

[4] G. Ferrari-Trecate, F.A. Cuzzola, D. Mignone, and M. Morari. Analysis of discrete-time piecewise affine and hybrid systems. *Automatica*, 38(12):2139–2146, 2002.

[5] M. F. Heertjes, S. van den Eijnden, B. Sharif, M. Heemels, and H. Nijmeijer. Hybrid Integrator-Gain System for Active Vibration Isolation with Improved Transient Response. *IFAC-PapersOnLine*, 52(15):454–459, 2019.

[6] J. P. Hespanha. *Linear systems theory*. Princeton university press, 2009.

[7] Z. Jiang and Y. Wang. Input-to-state stability for discrete-time nonlinear systems. *Automatica*, 37(6):857–869, 2001.

[8] Hasan K. Khalil. *Nonlinear Systems*. Prentice Hall, 3rd edition, 2002.

[9] M. Larsen and P. V. Kokotović. A brief look at the Tsypkin criterion: from analysis to design. *Int. J. Adapt. Control and Signal Processing*, 15(2):121–128, 2001.

[10] R. Middleton and J. Freudenberg. Non-pathological sampling for generalized sampled-data hold functions. *Automatica*, 31(2):315–319, 1995.

[11] D. Nešić, A.R. Teel, and P.V. Kokotović. Sufficient conditions for stabilization of sampled-data nonlinear systems via discrete-time approximations. *Syst. Control Lette.*, 38(4):259–270, 1999.

[12] D. Nešić, A.R. Teel, and E.D. Sontag. Formulas relating $\mathscr{KL}$ stability estimates of discrete-time and sampled-data nonlinear systems. *Syst. Control Lett.*, 38(1):49–60, 1999.

[13] B. Sharif, M. Heertjes, H. Nijmeijer, and W.P.M.H. Heemels. On the equivalence of extended and oblique projected dynamics with applications to hybrid integrator-gain systems. In *American Control Conference (ACC) 2021, New Orleans, USA*, pages 3434–3439, 2021.

[14] B. Sharif, M. F. Heertjes, and W. P. M. H. Heemels. Extended Projected Dynamical Systems with Applications to Hybrid Integrator-Gain Systems. In *2019 IEEE Conference on Decision and Control (CDC)*. IEEE, December 2019.

[15] E.D. Sontag. Smooth stabilization implies coprime factorization. *IEEE Transactions on Automatic Control*, 34(4):435–443, 1989.

[16] S. van den Eijnden, M. Francke, H. Nijmeijer, and M. F. Heertjes. Improving wafer stage performance with multiple hybrid integrator-gain systems. *IFAC-PapersOnLine*, 53(2):8321–8326, 2020.

[17] S van den Eijnden, W.P.M.H. Heemels, H. Nijmeijer, and M. Heertjes. Stability and performance analysis of hybrid integrator-gain systems: A linear matrix inequality approach. *Nonlinear Analysis: Hybrid Systems*, 45:101192, 2022.

[18] S. van den Eijnden, M. F. Heertjes, M. Heemels, and H. Nijmeijer. Hybrid Integrator-Gain Systems: A Remedy for Overshoot Limitations in Linear Control? *IEEE Control Systems Letters*, 2020.

[19] S. van den Eijnden, M. F. Heertjes, M. Heemels, and H. Nijmeijer. Frequency-domain tools for stability analysis of hybrid integrator-gain systems. In *European Control Conference, Rotterdam, The Netherlands*, 2021.

[20] S. van den Eijnden, M. F. Heertjes, and H. Nijmeijer. Robust stability and nonlinear loop-shaping design for hybrid integrator-gain-based control systems. In *American Control Conference, 2019*, pages 3063–3068, United States, 2019.

[21] D. van Dinther, B. Sharif, S. van den Eijnden, H. Nijmeijer, M. F. Heertjes, and M. Heemels. Overcoming performance limitations of linear control with hybrid integrator-gain systems. In *IFAC Conf. Anal. Design of Hybrid Systems (ADHS), Brussels, Belgium*, 2021.

[22] L. Zaccarian, D. Nešić, and A. R. Teel. First order reset elements and the Clegg integrator revisited. In *Proceedings of the 2005, American Control Conference, 2005.*, volume 1, pages 563–568, June 2005.